

Supplemental Material

Table S1. Primers used for real-time PCR

Gene	Primer	Product size (bp)
IL-6	sens: agttgccttcttgggactga revs: tccacgattcccagagaac	159
IL-1β	sens: gcccatcctctgtgactcat revs: agctcatatgggtccgacag	129
TNF-α	sens: agaagttcccaaattggcctc revs: ccacttggtggtttgctacg	120
IL-17	sens: tcctctgtgatctgggaag revs: ctcgaccctgaaagtgaagg	154
IL-23p19	sens: tgctggattgcagagcagtaa revs: gcatgcagagattccgagaga	121
β-actin	sens: agattactgctctggctcctagc revs: actcatcgactcctgcttget	147

Table S2. Primary and secondary antibodies used for immunofluorescence staining

Antibodies	Catalog No.	Dilution	Source
Mouse antimouse TLR2	ab 119333	1:200	Abcam
Rabbit antimouse TLR4	ab 13556	1:200	Abcam
Rat antimouse F4/80	ab 6640	1:500	Abcam
Rabbit antimouse IL-23P19	ab 45420	1:100	Abcam
Rabbit antimouse IL-17	ab 79056	1:100	Abcam
Rat antimouse CD3	ab 33429	1:100	Abcam
Rat antimouse TLR2	ab 11864	1:200	Abcam
Mouse antimouse βIII tubulin	ab 78078	1:200	Abcam
Rabbit antirat IgG Alexa Fluor 488	A21210	1:500	Invitrogen
Goat antirabbit IgG Alexa Fluor 568	A11011	1:500	Invitrogen
Goat antimouse IgG Alexa Fluor 647	A21236	1:500	Invitrogen

Table S3. Physiological parameters of mice before and after ICH

Parameter	Treatment group	Pre-ICH	1 days post-ICH	4 days post-ICH	7 days post-ICH
Temperature (°C)	ICH+vehicle	36.9±0.2	37.1±0.2	37.2±0.5	36.9±0.4
	ICH+SsnB	37.0±0.4	36.9±0.3	37.0±1.0	37.1±0.7
Peripheral white cell count (×10⁹/L)	ICH+vehicle	7.46±2.25	7.63±3.03	7.68±3.62	7.61±3.13
	ICH+SsnB	7.39±2.31	7.52±1.78	7.74±2.16	7.41±3.06

Figure S1.

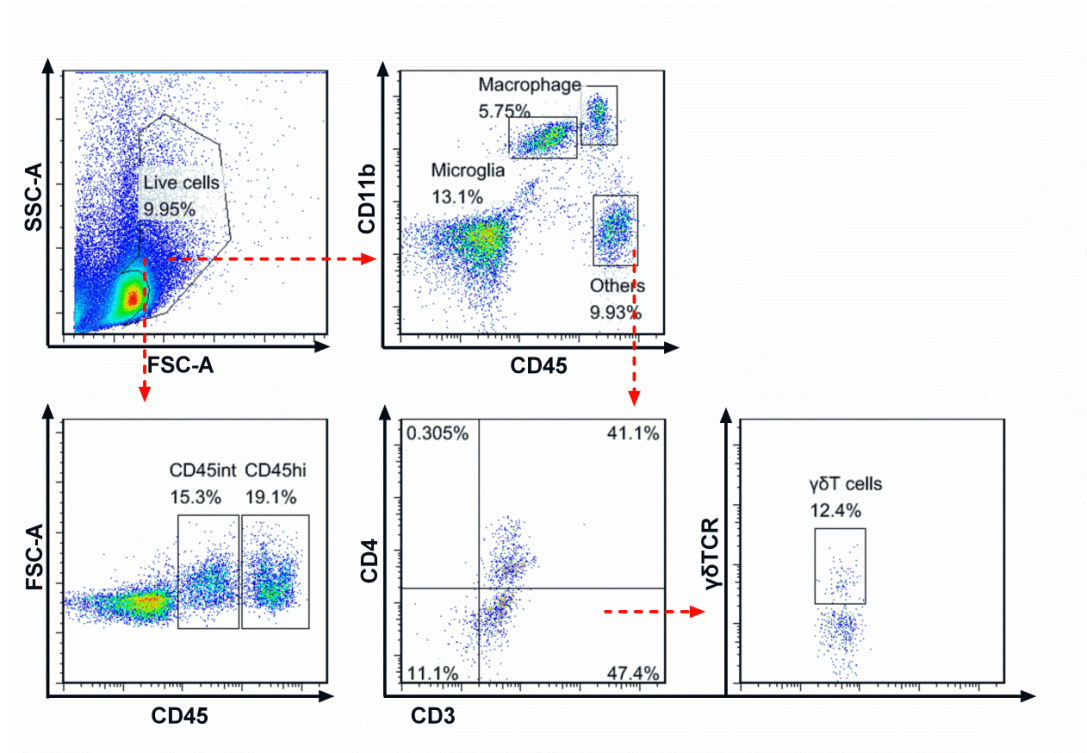


Figure S2.

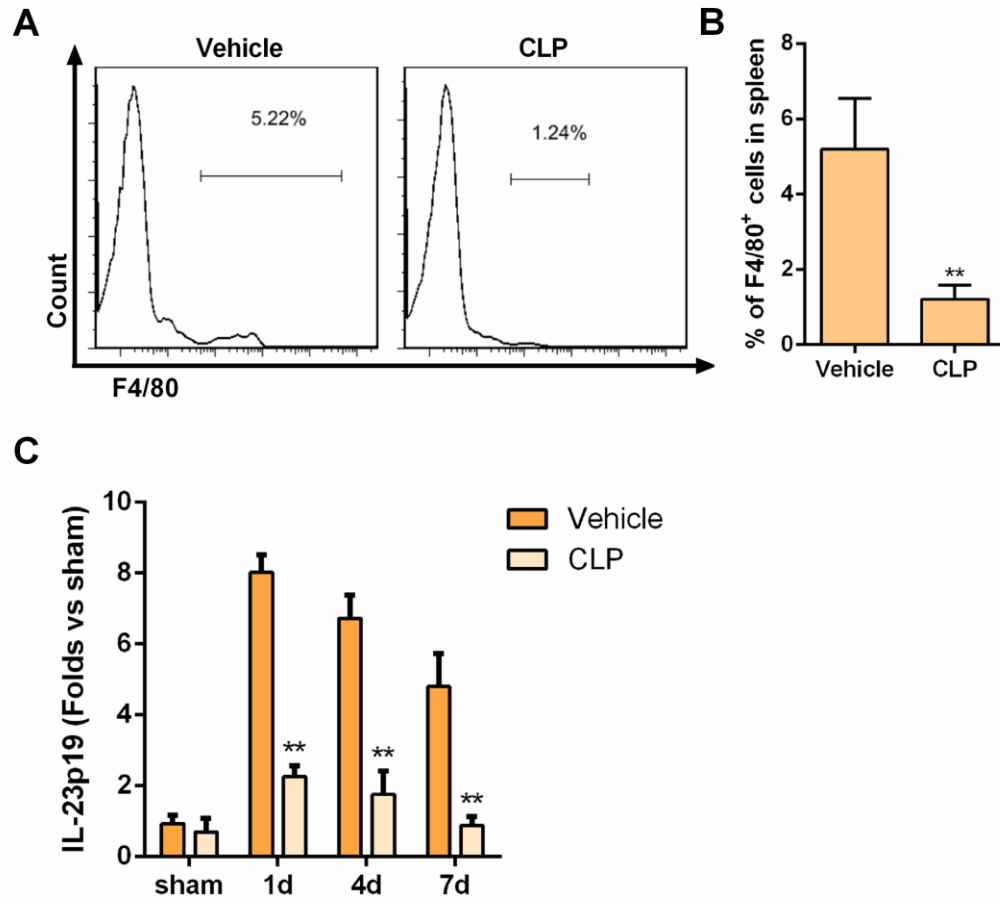


Figure S3.

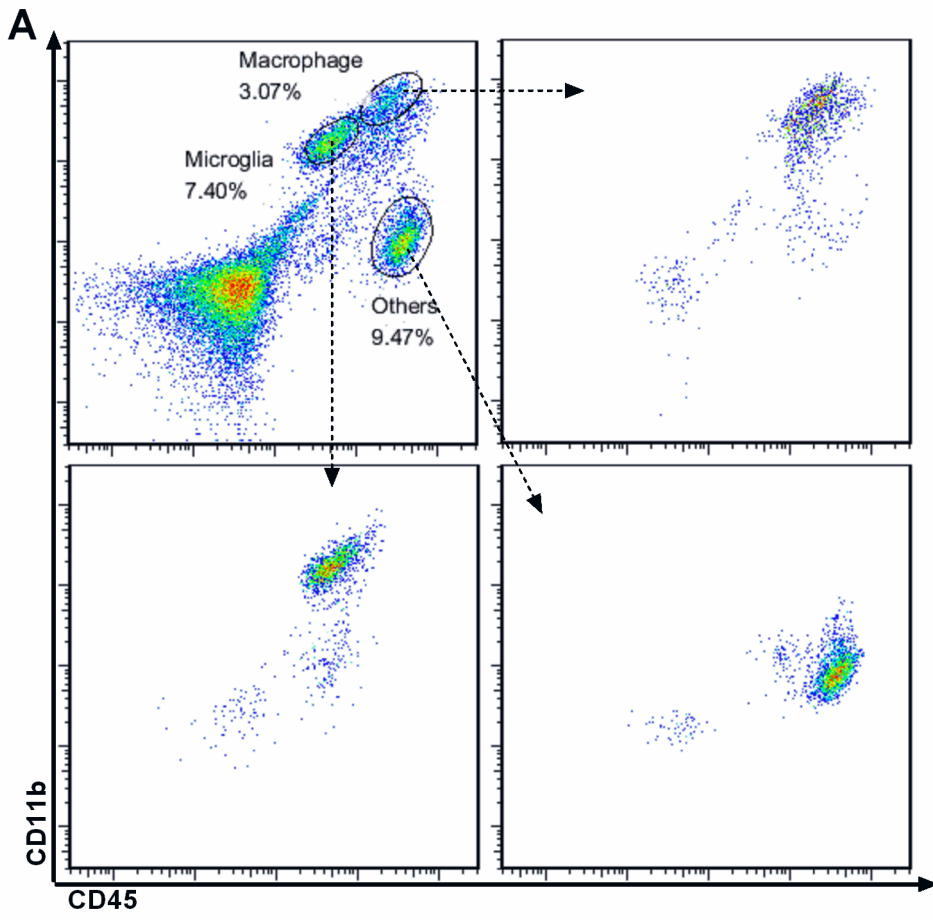


Figure S4.

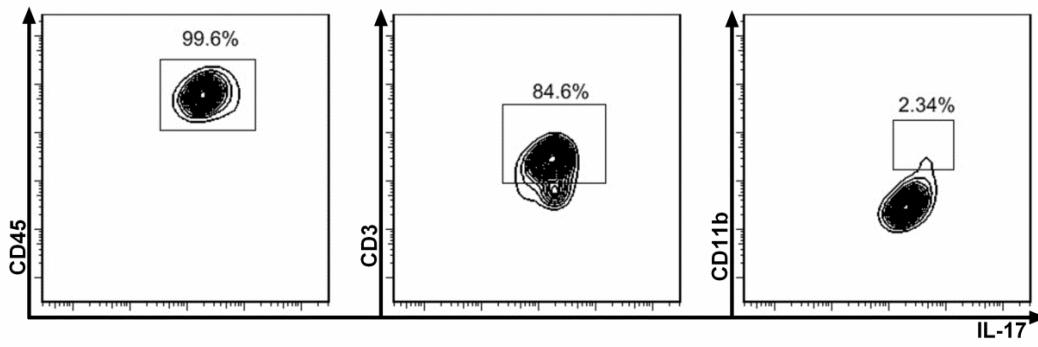


Figure S5.

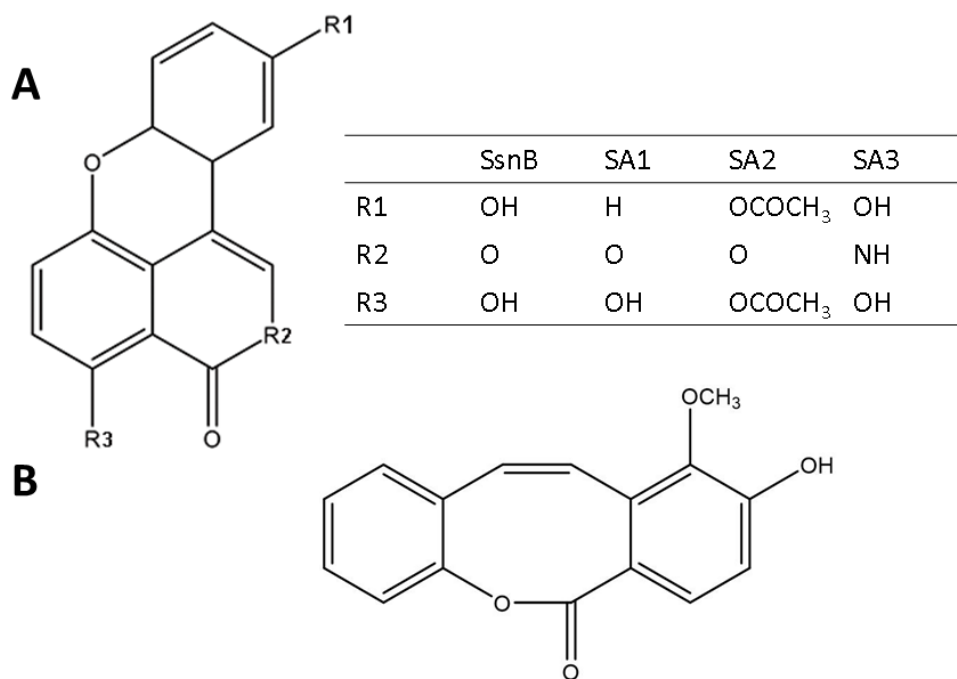
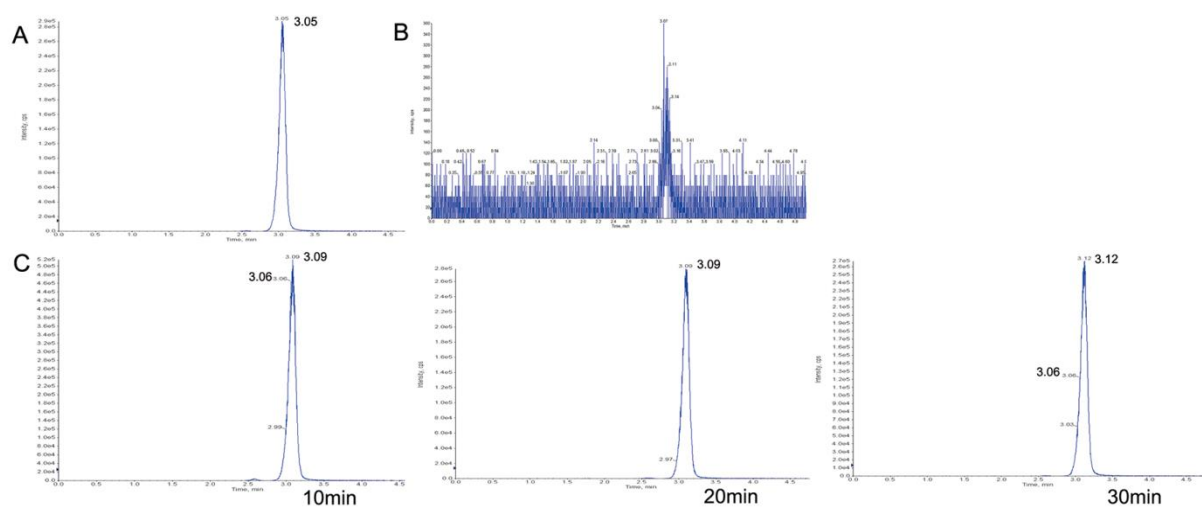


Figure S6.



Supplemental Figure Legends:

Figure S1. Macrophages, microglia, and other cell types were identified by FACS from pooled infiltrating inflammatory cells collected from 8 mice on day 4 after induction of ICH, according to the following markers: CD45^{high}CD11b^{high} cell were macrophages; CD45^{int}CD11b^{int} were microglia; CD45^{high}CD3⁺CD4⁺ cells were defined as brain-invading T helper cells; and CD45^{high}CD3⁺ cells were further analyzed to identify $\gamma\delta$ T lymphocytes. FSC-A, forward scatter channel area; SSC-A, side scatter channel area.

Figure S2. Depletion of macrophages in the spleen upon clodronate liposome (CLP) treatment. (A) Percentages of F4/80⁺ macrophages in spleens of vehicle-treated and CLP-treated mice at 1 day after ICH determined by flow cytometric analysis. (B) Quantified percentages of F4/80⁺ macrophages in spleens of vehicle-treated and CLP-treated groups. (**p<0.01 vs. vehicle, n=5). (C) mRNA expression of IL-23p19 in perihematoma tissues at 1, 4, and 7 days after ICH in the CLP- and vehicle-treated mice. (**p<0.01 vs. vehicle, n=4).

Figure S3. Sorting of macrophages, microglia, and other cells from pooled infiltrating inflammatory cells collected from 7 mice at day 4 by FACS for subsequent evaluation of IL-23p19 expression. CD45^{high}CD11b^{high} cell were macrophages; CD45^{int}CD11b^{int} were microglia; and CD45⁺, CD11b⁻ were grouped as “other” cells.

Figure S4. CD3⁺ T lymphocytes were the main source of IL-17. The indicated surface markers were used to identify IL-17-producing cells among pooled infiltrating inflammatory cells collected from 8 mice on day 4 after induction of ICH and sorted by FACS.

Figure S5. (A) Structures of SsnB and the compounds derived from SsnB. (B) Structure of J1, the isomeric isomer of SsnB.

Figure S6. SsnB crosses the mouse blood-brain barrier. (A) Standard curve for SsnB. (B) SsnB concentrations in cerebral tissues of mice subjected to ICH and in the vehicle-treated group. (C) SsnB concentrations in cerebral tissues of ICH model mice at 10, 20, and 30 minutes after intravenous injection of SsnB.